**Atmospheric
Chemistry
and Physics
Discussions**

Sources of anions in aerosols in northeast Greenland during late winter

**M. Fenger[1], L. L. Sørensen[2], K. Kristensen[1], B. Jensen[2], Q. T. Nquyen[1,2],
J. K. Nøjgaard[2], A. Massling[2], H. Skov[2,3], and M. Glasius[1]**

[1]Department of Chemistry, Aarhus University, 8000 Aarhus, Denmark
[2]Department of Environmental Science, Aarhus University, 4000 Roskilde, Denmark
[3]Institute of Chemical Engineering, Biotechnology and Environmental Technology, University of Southern Denmark, 5230 Odense M, Denmark

Correspondence to: L. L. Sørensen (lls@dmu.dk)

Discussion Paper | Discussion Paper | Discussion Paper | Discussion Paper | Discussion Paper

ACPD

12, 14813–14836, 2012

Sources of anions in aerosols in northeast Greenland during late winter

M. Fenger et al.

Title Page

Abstract	Introduction
Conclusions	References
Tables	Figures

◄ | ►|

◄ | ►

Back | Close

Full Screen / Esc

Printer-friendly Version

Interactive Discussion

Sources of anions in aerosols in northeast Greenland during late winter

M. Fenger et al.

Abstract

The knowledge of climate effects of atmospheric aerosols is associated with large uncertainty, and a better understanding of their physical and chemical properties is needed, especially in the Arctic environment. The objective of the present study is to improve our understanding of the processes affecting the composition of the aerosols in the high Arctic. Therefore size-segregated aerosols were sampled at a high Arctic site, Station Nord (Northeast Greenland), in March 2009 using a Micro Orifice Uniform Deposit Impactor. The aerosol samples were extracted in order to analyze the three water-soluble anions: chloride, nitrate and sulphate. The results are discussed based on possible chemical and physical transformations as well as transport patterns.

The total concentrations of the ions at Station Nord were 53–507 ng m^{-3}, 2–298 ng m^{-3} and 535–1087 ng m^{-3} for chloride (Cl$^-$), nitrate (NO$_3^-$) and sulphate (SO$_4^{2-}$), respectively. The aerosols in late winter/early spring, after polar sunrise, are found to be a mixture of long-range transported and regional to local originating aerosols. Fine particles, smaller than 1 μm, containing SO$_4^{2-}$, Cl$^-$ and NO$_3^-$, are hypothesized to originate from long-range transport, where SO$_4^{2-}$ is by far the dominating anion accounting for 50–85 % of the analyzed mass. The analysis suggests that Cl$^-$ and NO$_3^-$ in coarser particles (>1.5 μm) originate from local/regional sources. Under conditions where the air mass is transported over sea-ice at high wind speeds, very coarse particles (>18 μm) are observed and it is hypothesized that frost flowers on the sea ice is a source of very coarse chloride particles in the Arctic.

1 Introduction

The changing climate is of increasing concern among politicians, scientists and the general population. There are still many important climatic subjects, where the knowledge is insufficient (IPCC, 2007). The largest temperature increase, due to climate change, is observed in the high Arctic, where the observed temperature increase is

twice as high as at mid latitude, and the increase is expected to continue in future climates (ACIA, 2004; Quinn et al., 2008). Therefore an enhanced understanding of the climate dynamics in this particular area is highly needed; however measurements and studies of the atmospheric chemistry in high Arctic are still very limited.

The presence of aerosols in the atmosphere affects the environment in multiple ways. One of the most significant effects is the scattering of incoming solar radiation resulting in a net cooling of air and thereby offsetting some of the global warming induced by greenhouse gases. However, the climate forcing from aerosols still requires focus and in-depth studies since it is one of the largest uncertainties in predicting future climate by models according to the Intergovernmental Panel on Climate Change (IPCC, 2007). These studies are complicated by the fact that the physical and chemical properties of aerosols are highly variable in both time and space.

Aerosols contain a number of chemically different species influencing their optical and cloud-nucleating properties depending on their origin and travel "history" which determine the possible transformation processes. The effect of individual particle properties on the scattering efficiency of an atmospheric layer, or on cloud albedo, depends on the size segregated chemical composition of the atmospheric aerosol. Water-soluble inorganic anions strongly determine the sub-saturated growth of particles under atmospheric conditions and their ability to form clouds (e.g. Swietlicki et al., 2008).

About three decades ago, it was discovered that during winter, a considerable part of the Arctic atmosphere becomes highly polluted because of the accumulation of Eurasian pollutants, creating what became generally known as the "Arctic Haze" (Flyger et al., 1980; Barrie et al., 1981; Heidam et al., 2004; Glasow and Crutzen, 2007). Arctic haze aerosols consist primarily of sulphate (SO_4^{2-}) and particulate organic matter in addition to ammonium (NH_4^+), nitrate (NO_3^-) and black carbon (BC) (e.g. Li and Barrie, 1993; Quinn et al., 2002). The Arctic haze phenomenon results in a characteristic annual variation of sulphate, nitrate and anthropogenically derived elements (e.g. Heidam et al., 2004; Quinn et al., 2007). Concentrations of aerosols in the high Arctic are at their highest during late winter and early spring when anthropogenic pollution is

Sources of anions in aerosols in northeast Greenland during late winter

M. Fenger et al.

Title Page

Abstract	Introduction
Conclusions	References
Tables	Figures

◄◄   ►►

◄   ►

Back   Close

Full Screen / Esc

Printer-friendly Version

Interactive Discussion

most efficiently transported from lower latitudes (e.g. Heidam, et al. 2004) to the Arctic. Thus combustion sources at other continents influence and partly determine the composition of the observed aerosols in the high Arctic. Late winter and early spring is also accompanied by significant increases in the amount of solar radiation reaching the surface and initiating the photochemistry in the Arctic atmosphere and at/in the snowpack; the latter leading to enhanced emission of gases from the snow (Domine and Shepson, 2002). Therefore both long-range transport and local processes influence the composition of the Arctic aerosols, and subsequently the system becomes very complex. It is important to obtain a better understanding of the physical and chemical dynamics of the particles in the Arctic region.

In this paper we present the size fractionated main inorganic components: Cl^-, NO_3^- and SO_4^{2-} in aerosols measured at a high Arctic site in northeast Greenland. The sampling of size-segregated aerosols was performed shortly after polar sunrise. The objective is to improve the understanding of the processes influencing the chemical composition of aerosols in the high Arctic atmosphere by discussing the results as a function of sources, physical and chemical transformations as well as transport patterns.

2   Method

2.1   Logistics

Atmospheric measurements were carried out at Station Nord first time in the late 1970s (Flyger et al., 1980) and have taken place continuously since the late 1990s (Heidam et al., 2004). Station Nord is located in a remote area in northeast Greenland at 81°36′ N, 16°40′ W (Fig. 1a). It is a small military installation inhabited by a permanent staff of five, and with relatively few guests (scientists and others) throughout the year, and mainly during summer.

The sampling site, Flygers Hut, is located approximately 2 km south of the main complex of the buildings at an altitude of 25 m a.s.l. (Fig. 1b). The area is a fairly flat

peninsula of about 10 km × 10 km. In winter periods, Station Nord is recurrently exposed to air masses coming from northern and eastern direction from Eurasia (Heidam et al., 1999).

Aerosols were sampled from 5 to 24 March 2009 just after the polar sunrise. The length of the days increased rapidly, with the sun above the horizon for a few minutes in the beginning of the sampling period, to 20 h a day in the end. Throughout the sampling period the temperature was on average −40 °C varying between −18 °C and −45 °C. The wind speed ranged between 1–8 m s^{-1} except during night 13 March, on 16–17 March and on 21 March when the wind speed reached 10 m s^{-1}. The measurements of wind speed at station North is carried out by the use of cup anemometers, which often freeze at low temperatures and therefore the uncertainty of wind speed measurements is large. Here we use reanalysis data from NCEP/DOE AMIP-II (Kanamitsu et al., 2002) for wind speed estimates at 1000 millibar (Fig. 2) recognizing that these data are also associated with large uncertainty, especially in the Arctic. Comparing reanalysis data to measured data, using a sonic anemometer (METEK-USA) in spring 2011 (Fig. S1), shows weak correlation ($R^2 = 0.38$). However the measured and modelled data generally show the same trend in the magnitude of the wind speed. The wind speed data are estimated at 1000 millibar and the ground pressure were at times lower during the measurement campaign yet comparing wind speeds for 1000, 925 and 800 millibar shows no big difference in the wind speed.

2.2 Sampling and analysis

The collection of size-segregated aerosols was conducted by a Micro Orifice Uniform Deposit Impactor (MOUDI), MSP Corporation, Model 110-R at a flow rate of 30 l min^{-1}. The sampler was operated with 11 fractionation stages and the aerodynamic cut-off diameters (particle sizes corresponding to the 50 % collection efficiency) of the stages are 18, 10.0, 5.6, 3.2, 1.8, 1.00, 0.56, 0.32, 0.18, 0.100 and 0.056 µm. In order to reduce particle bouncing the aluminium sampling foils were coated with silicone spray before sampling. The foils were changed 9 times during the collection period and the length of

each sample period varied from 22 to 71 hours. Sample blanks were included for each collection period. This was represented by a foil that was handled like a sample foil, except that it was not placed in the MOUDI. The aerosol samples were stored in clean plastic vials and shipped to the laboratory under freezing conditions. In the laboratory

5   samples were stored in darkness at −20 °C until analysis.

The MOUDI foils were ultrasonically extracted in 6 ml distilled water for 2 h. The extracts were filtered with a syringe filter (0.22 µm pore size) followed by analysis of the major anions: Cl^-, NO_3^- and SO_4^{2-} using a Metrohm suppressed ion chromatography system. A Metropsep A Supp 5–250 column was used with an eluent of

10   3.2 mM Na_2CO_3/1.0 mM $NaHCO_3$. An auto sampler injector was used to introduce 20 µl of sample into the eluent maintained at a flow rate of 0.7 ml min^{-1}. In addition, blank foils were extracted for each analysis and the blank concentrations were subtracted from the sample values. Detection limits were 0.55 ng m^{-3} for Cl^-, 0.40 ng m^{-3} for NO_3^- and 0.32 ng m^{-3} for $SO_4^{2-}$for three day sampling and three times higher for one day

15   sampling periods. The size intervals of the sampled aerosol are not equally distributed thus in order to illustrate the aerosol size distribution the concentration of particles are normalized. The normalized concentrations $dC/dlogD_p$ is given by Eq. (1).

$$\frac{dC}{d \log D_p} = \frac{C}{\log \sqrt{\frac{d_{p,\text{bigger than}}}{d_{p,\text{smaller than}}}}} \tag{1}$$

Where C is the concentration found on the stage, and d_p is the diameters for the stage

20   size boundaries used.

A Scanning Mobility Particle Sizer (SMPS, Model: TSI DMA 3081, TSI CPC 3010) was operated during the MOUDI sampling periods. The SMPS inlet was connected to the station inlet system, which is operated by drawing an air flow of 1 m^3 min^{-1} through a stainless steel tubing system with a diameter of 0.10 m into the hut. This inlet has no

25   cut-off for atmospheric particles. The SMPS sampling time was set to 2.5 min. and data were further averaged for the corresponding MOUDI sampling periods. Based on the

obtained particle number size distributions, the particle volume size distributions were calculated in the size regime between 10–400 nm assuming spherical particles. Then, the particulate mass was estimated using an average particle density of 1.2 g cm^{-3}.

During the field campaign concentrations of NO$_x$ (NO$_2$ and NO) was estimated as half hour mean based on continuous measurements using a chemiluminiscent monitor (API NO$_x$ analyzer, model 200AU) at a precision of ±5 %. The NO$_x$ and NO concentrations during the field campaign are shown in Fig. 3.

3 Results and discussion

Table 1 displays the concentrations of the major ions (Cl$^-$, NO$_3^-$ and SO$_4^{2-}$) for 11 size segregated stages of MOUDI samples. The concentrations range between 53–507 ng m^{-3}, 2–298 ng m^{-3} and 535–1087 ng m^{-3} for Cl$^-$, NO$_3^-$ and SO$_4^{2-}$, respectively, and contribute to about 6–39 %, 0.3–25 % and 50–85 % of the analyzed mass. The standard deviation ranges between 4–15 ng m^{-3} for Cl$^-$, between 4–14 ng m^{-3} for NO$_3^-$ and between 7–25 ng m^{-3} for SO$_4^{2-}$. The measured concentrations are comparable to findings observed at other Arctic sites e.g. at Svalbard and Alert (Kawamura et al., 2007; Teinila et al., 2003). The normalized size-segregated mass distributions of SO$_4^{2-}$, Cl$^-$, and NO$_3^-$ are shown in Fig. 4, 5 and 6.

Several parameters are important with respect to aerosol mass concentration, particle number concentration and size distribution. These include emission strengths, short- and long-range transport, meteorological conditions and physical as well as chemical processes, which control the formation of secondary aerosols and their changes at a later stage.

Submicron particles from 0.1 to 1 µm constitute the main mass of long-range transported particles (Seinfeld and Pandis, 2006) and a large part of the particles we collected are associated to this size fraction. The Hybrid Single Particle Lagrangian Integrated Trajectory (HYSPLIT) model was used to generate air-mass back trajectories in

order to estimate the history of the observed aerosols. Back trajectories were calculated arriving at 50 and 500 m a.s.l. every 12 h (Fig. 7).

From the back trajectories, three main classes of air mass origin were observed during the sampling period: (1) west of Station Nord (Canada, West Greenland and the North Pole (P1 and P2) and (2) north of Station Nord (the North Pole and Siberia (P3, P4, P8 and P9)) and (3) along the coast of North Greenland (P5, P6 and P7) (see Fig. 7). The three classes of air masses are all characterized by transport over ice/snow covered areas, however, transport over pure sea ice was longer during the sampling periods P3, P4, P8 and P9 and the atmosphere also seemed to be more stable with less vertical mixing for those periods.

The sources of local pollution can be considered to be negligible because of the remote location and the minimum of influence from inhabitants at Station Nord throughout the year.

The particle mass size distributions of SO_4^{2-} have a predominant mode in the fine fraction (<1 μm), peaking approximately at a mean geometric diameter (Dg) of 0.32 μm. In contrast to Cl^- and NO_3^- the particle mass size distribution profile of SO_4^{2-} is constant even though the origin of air mass changes for the different sampling periods according to back trajectory analysis with HYSPLIT. This suggests that the majority of the SO_4^{2-} is long range transported and originates from combustion sources, which also supports previous results from Heidam et al. (2004) and is supported by the observed correlation between SO_4^{2-} and black carbon (Grube et al., 2012). SO_4^{2-} is by far the dominating anion during the collection period and with Dg of approximately 0.32 μm this size may have a considerable climatic effect depending on its mixing state with other species, since visible solar radiation is scattered very efficiently within this size range (Wallace and Hobbs, 2006). The coarser mode (>1 μm) SO_4^{2-} particles, found with smaller mass concentrations, may originate from sea spray and/or SO_4^{2-} formed on coarse sea salt or soil particles. However the large particle size suggests that this is not long-range transported but is originating from a nearby source. The contribution from sea salt sulphate (ss-SO_4^{2-}) at Station Nord is small according to Heidam et al. (2004),

Title Page

Abstract | Introduction

Conclusions | References

Tables | Figures

⏮ | ⏭

◀ | ▶

Back | Close

Full Screen / Esc

Printer-friendly Version

Interactive Discussion

which is consistent with other studies (Rankin et al., 2002), where it was found that sulphate is depleted in freezing ice due to formation of mirabilite (Na_2SO_4 $10H_2O$). Of the three analyzed anions, SO_4^{2-} is however the major component accounting for the highest mass concentrations of about 50–85 % of the analyzed mass. Studies in Alaska have found about 30 % of the total mass being SO_4^{2-} in Arctic aerosols during winter-time (Barrie et al., 1981). The fraction of SO_4^{2-} in the size range 56–560 nm to the total mass varies from 7–65 % of the total aerosol mass, which is calculated based on SMPS measurements. This result is in accordance with the observations of Barrie et al. (1981). Submicron SO_4^{2-} particles consist primarily of non-sea-salt sulphate formed by gas-to-particle conversion of the photo-oxidation products of e.g. SO_2 and dimethylsulphide.

As described previously, Station Nord is placed on a peninsula and surrounded by sea. The fact that the surrounding ocean was covered with ice during the sampling period may have reduced the likelihood of atmospheric direct sea spray emissions reaching Station Nord. The lifetime of coarse aerosols is confined due to gravitational settling so only aerosols with diameters slightly below 1 µm make their way to Station Nord from distant sources. Sea ice maps calculated from The Advanced Microwave Scanning Radiometer for EOS (AMSR-E) data using the ARTIST (Arctic Radiation and Turbulence Interaction Study) sea ice algorithm (ASI 5) (www.seaice.de) (Fig. 8) show that the ice-cover extent does not change considerably during the sampling period in the Arctic area. This means that the distance from the sampling site to open water remains constant at approximately 1000 km during the field study. It is likely that Cl^- and NO_3^- have more local origins, since the size distribution profiles differ from SO_4^{2-}, and are found in the larger fractions, however splitting the sampling period into three major episodes, reveal size distribution profiles more comparable for all the ions in air masses originating from west, with less exposure to sea ice. This suggests that part of the Cl^- and NO_3^- is also long-range transported.

The particle mass size distributions of Cl^- consist of at least 3 modes, with maxima at diameters of $D = 0.56$ µm, 1–1.8 µm and >18 µm. It is expected that the aerosols

undergo transformation during their transport to Station Nord. Cl^- in the fine fraction can originate from Cl^- on coarser particles, which is released into the gas phase during transport, due to reactions between sea salt and acidic species or their precursors (e.g. Barrie and Barrie, 1990; Fischer, 2001; Hillamo et al., 1998; Teinila et al., 2003; Quinn et al., 2009). This reaction induces a redistribution of Cl^- from the coarse to the fine fractions. This process is supported by the fact that the finest mode is here found to be associated with the long-range transported SO_4^{2-} while the larger size fractions are likely to have other origins.

A closer analysis of Cl^- profiles (Fig. 5) shows that during transport from Canada and west Greenland (P1 and P2), Cl^- is mainly associated with long-range transported submicron particles, shifting to dominance of super micron particles when the air mass arrives directly from the sea ice (P3 and P4). Then the wind direction changes, and air masses are again transported along the coast from west Greenland revealing a mixture of submicron and super-micron Cl^- particles, with very coarse particles (>18 µm) in P7. The Cl^- profiles change into dominance from super micron particles when the air mass again arrives from the frozen ocean (P8 and P9). An explanation of the observed mass concentrations of Cl^- in the different size regimes, could be re-fractionation of the aerosol sizes distribution, during transport across the ice-covered ocean, combined with new contribution of aerosols/gases from frost flowers and refreezing leads. This is consistent with the more varying fractionation for the samples during the periods P3, P4, P8 and P9, where the air mass has been transported over sea ice for a longer time and, according to HYSPLIT back trajectories, had less vertical mixing. It has been suggested by (Wolff et al., 2003) that frost flowers can contribute to wind transport of sea salt and (Domine et al., 2004) found wind transported Cl^- from open sea to snow. However, the measurements by Domine et al. (2004) were carried out in areas with a short distance to open water. The sample collected from March 20th to March 22nd (P7) revealed a large amount of Cl^- on the very coarse particles. On the 20 March the wind speed was high and the air mass was transported over sea-ice. These very coarse particles can only originate from local sources as their sedimentation velocity

does not allow transport over thousands of kilometres. We hypothesize that Cl^- on the very coarse particles originates from frost flowers possibly torn at high wind speeds. Conversely, (Roscoe et al., 2011) found that frost flowers grown in the laboratory do not break even at high wind speeds ($12\,m\,s^{-1}$), on the other hand the atmospheric humidity in the laboratory experiments was not low as it is in the Arctic, and there were no blowing snow, or other particles, in the laboratory tank either. Another possible explanation could be that Cl^- simply is taken up by wind blown snow when the air mass is passing over the frost flowers.

The size distributions of NO_3^- are dominated by at least 4 modes with maxima at geometric mean diameter of $Dg = 0.18\,\mu m$, 0.56–$1.8\,\mu m$, 3.2–$5.6\,\mu m$ and $>18\,\mu m$. Over the oceans the particle mass size distribution of NO_3^- typically follows the surface area distribution of sea salt (Prospero, 2002). Like SO_4^{2-} and Cl^- the fine mode of NO_3^- is likely originated from long-range transport and mass contributions in the coarser size regime originate from local sources. Recent studies by (Douglas et al., 2012) show high NO_3^- concentrations in frost flowers and surface brine, suggesting that NO_3^- can be emitted from frost flowers. In contrast to Cl^- and SO_4^{2-}, NO_3^- shows a significant mode in the size regime $Dg = 3.2$–$5.6\,\mu m$ between the 16 March and 17 March (P5). During these days the wind was higher than average (7–$9\,m\,s^{-1}$), which maybe is too low for destroying frost flowers, but this could influence the snowpack, leading to enhanced emissions from the snowpack. According to (Domine and Shepson, 2002; Douglas et al., 2012) the snow contains NO_3^-, thus NO_3^- could be released directly as particles in wind blown snow under conditions with increasing wind speeds. However Cl^- is also found at elevated concentrations in the surface snow over sea ice (Douglas et al., 2012) and if the increased NO_3^- concentration in the larger particles were due to wind blown snow we would expect an increase in Cl^- concentration in this size range as well.

According to (Grannas et al., 2007) high concentrations of NO_x can be found in the snowpack and NO_2 emitted from the snow followed by oxidation in the atmosphere

could explain the NO_3^- in the different size fractions in P5. Prior to the episode P5, the NO_x concentration in the atmosphere was increased (see Fig. 3).

4 Conclusions

The primary objective of this study was to improve the current understanding of the composition and origin of Arctic aerosols through analysis of mass size distributions of major anions in late winter Arctic aerosols at Station Nord, northeast Greenland. It was found that the aerosols in late winter/early spring just after polar sunrise are a mixture of long-range transported and regional to local originating aerosols. Fine particles, smaller than 1 µm containing SO_4^{2-}, Cl^- and NO_3^-, most probably originate from long-range transport, which appears to be the most important source of major inorganic anions at Station Nord, where SO_4^{2-} is by far dominating, accounting for 50-85 % of the analyzed mass. The analysis suggests that Cl^- and NO_3^- in coarser particles (>1.5 µm) originate from local/regional sources. Under conditions where the air mass is transported over sea-ice at high wind speeds very coarse particles (>18 µm) are found, and it is hypothesized that frost flowers on the sea-ice is a source to Cl^- and NO_3^- particles in the Arctic. This is supported by (Shaw et al., 2010), who found that particles in the Arctic in winter clearly had a sea spray profile despite the frozen polar ocean. The uncertainties of the NO_3^- sources are still substantial and further studies on nitrogen processes in the high Arctic are needed.

Supplementary material related to this article is available online at: http://www.atmos-chem-phys-discuss.net/12/14813/2012/ acpd-12-14813-2012-supplement.pdf.

Title Page

Abstract | Introduction

Conclusions | References

Tables | Figures

◄ | ►

◄ | ►

Back | Close

Full Screen / Esc

Printer-friendly Version

Interactive Discussion

References

ACIA (Arctic Climate Impact Assessment): Overview Report, Cambridge Univ. Press, Cambridge, 140 pp., 2004.

Barrie, L. A. and Barrie, M. J.: Chemical-Components of Lower Tropospheric Aerosols in the High Arctic – 6 Years of Observations, J. Atmos. Chem., 11, 211–226, 1990.

Barrie, L. A., Hoff, R. M., and Daggupaty, S. M.: The influence of mid-latitudinal pollution sources on haze in the Canadian arctic, Atmos. Environ., 15, 1407–1419, 1981.

Domine, F. and Shepson, P. B.: Air-snow interactions and atmospheric chemistry, Science, 297, 1506–1510, 2002.

Domine, F., Sparapani, R., Ianniello, A., and Beine, H. J.: The origin of sea salt in snow on Arctic sea ice and in coastal regions, Atmos. Chem. Phys., 4, 2259–2271, doi:10.5194/acp-4-2259-2004, 2004.

Douglas, T. A., Domine, F., Barret, M., Anastasio, C., Beine, H. J., Bottenheim, J., Grannas, A., Houdier, S., Netcheva, S., Rowland, G., Staebler, R., and Steffen, A.: Frost flowers growing in the Arctic ocean-atmosphere-sea ice-snow interface: 1. Chemical composition, J. Geophys. Res., 117, doi:10.1029/2011JD016460, D00R09, 2012.

Fischer, H.: Imprint of large-scale atmospheric transport patterns on sea-salt records in northern Greenland ice cores, J. Geophys. Res.-Atmos., 106, 23977–23984, 2001.

Flyger, H., Heidam, N. Z., Hansen, K. A., Rasmussen, L., and Megaw, W. J.: The background levels of the summer tropospheric aerosol and trace gases in Greenland, J. Aerosol Sci., 11, 95–110, 1980.

Glasow, R. and Crutzen, P. J.: Tropospheric Halogen Chemistry in: The Atmosphere, edited by: Russel and Keeling, ISBN:9780080450919, Elsevier, 2007.

Grannas, A. M., Jones, A. E., Dibb, J., Ammann, M., Anastasio, C., Beine, H. J., Bergin, M., Bottenheim, J., Boxe, C. S., Carver, G., Chen, G., Crawford, J. H., Dominé, F., Frey, M. M., Guzmán, M. I., Heard, D. E., Helmig, D., Hoffmann, M. R., Honrath, R. E., Huey, L. G., Hutterli, M., Jacobi, H. W., Klán, P., Lefer, B., McConnell, J., Plane, J., Sander, R., Savarino, J., Shepson, P. B., Simpson, W. R., Sodeau, J. R., von Glasow, R., Weller, R., Wolff, E. W., and Zhu, T.: An overview of snow photochemistry: evidence, mechanisms and impacts, Atmos. Chem. Phys., 7, 4329–4373, doi:10.5194/acp-7-4329-2007, 2007.

Grube, A.G., Skov, H., Christensen, J. H., Jensen, B., Nquyen, Q. T., Nøjgaard, J. K., Sørensen, L. L., and Massling, A.: Implication of black carbon and sulphate mass concentrations in Northeast Greenland: a comparison of measurements and model results, submitted, 2012.

Heidam, N. Z., Wåhlin, P., and Christensen, J. H.: Tropospheric Gases and Aerosols in Northeast Greenland, J. Atmos. Sci., 56, 261–278, 1999.

Heidam, N. Z., Christensen, J., Wåhlin, P., and Skov, H., Arctic atmospheric contaminants in NE Greenland: levels, variations, origins, transport, transformations and trends 1990ΓÇô2001, Science of the Total Environment, 331, 5-28, 2004.

Hillamo, R., Allegrini, I., Sparapani, R., and Kerminen, V. M.: Mass size distributions and precursor gas concentrations of major inorganic ions in Antarctic aerosol, Int. J. Environ. An. Ch., 71, 353–372, 1998.

IPCC: Climate Change 2007: Contribution of Working Group I to the Fourth Assessment Report of the Intergovernmental Panel on Climate Change, edited by: Solomon, S., Qin, D., Manning, M., Chen, Z., Marquis, M., Averyt, K. B., Tignor, M., and Miller, H. L., Cambridge University Press, Cambrigde, UK and New York, NY, USA, 996 pp., 2007.

Kanamitsu, M., Ebisuzaki, W., Woollen, J., Yang, S. K., Hnilo, J. J., Fiorino, M., and Potter, G. L.: Ncep-Doe Amip-Ii Reanalysis (R-2), Bull. Amer. Meteor. Soc., 83, 1631–1643, 2002.

Kawamura, K., Narukawa, M., Li, S. M., and Barrie, L. A., Size distributions of dicarboxylic acids and inorganic ions in atmospheric aerosols collected during polar sunrise in the Canadian high Arctic, J. Geophys. Res.-Atmos., 112, doi:1029/2006JD008244, D10307, 2007.

Li, S. M. and Barrie, L. A.: Biogenic Sulfur Aerosol in the Arctic Troposphere .1. Contributions to Total Sulfate, J. Geophys. Res.-Atmos., 98, 20613–20622, 1993.

Prospero, J. M.: The chemical and physical properties of marine aerosols: An introduction, Springer-Verlag Berlin, Berlin, Germany, 82 pp. 2002

Quinn, P. K., Bates, T. S., Baum, E., Doubleday, N., Fiore, A. M., Flanner, M., Fridlind, A., Garrett, T. J., Koch, D., Menon, S., Shindell, D., Stohl, A., and Warren, S. G.: Short-lived

Title Page

Abstract | Introduction

Conclusions | References

Tables | Figures

◄ | ►|

◄ | ►

Back | Close

Full Screen / Esc

Printer-friendly Version

Interactive Discussion

pollutants in the Arctic: their climate impact and possible mitigation strategies, Atmos. Chem. Phys., 8, 1723–1735, doi:10.5194/acp-8-1723-2008, 2008.

Quinn, P. K., Miller, T. L., Bates, T. S., Ogren, J. A., Andrews, E., and Shaw, G. E.: A 3-year record of simultaneously measured aerosol chemical and optical properties at Barrow, Alaska, J. Geophys. Res.-Atmos., 107, doi:10.1029/2001JD001248, 4130, 2002.

Quinn, P. K., Shaw, G., Andrews, E., Dutton, E. G., Ruoho-Airola, T., and Gong, S. L.: Arctic haze: current trends and knowledge gaps, Tellus B, 59, 99–114, 2007.

Quinn, P. K., Bates, T. S., Schulz, K., and Shaw, G. E.: Decadal trends in aerosol chemical composition at Barrow, Alaska: 1976–2008, Atmos. Chem. Phys., 9, 8883–8888, doi:10.5194/acp-9-8883-2009, 2009.

Rankin, A. M., Wolff, E. W., and Martin, S., Frost flowers: Implications for tropospheric chemistry and ice core interpretation, J. Geophys. Res.-Atmos., 107, 2002.

Roscoe, H. K., Brooks, B., Jackson, A. V., Smith, M. H., Walker, S. J., Obbard, R. W., and Wolff, E. W., Frost flowers in the laboratory: Growth, characteristics, aerosol, and the underlying sea ice, J. Geophys. Res., 116, doi:10.1029/2010JD015144, D12301, 2011.

Seinfeld, J. H. and Pandis, S. N.: Atmospheric Chemistry and Physics – From Air Pollution to Climate Change, 2nd. edn. Wiley, 2006.

Shaw, P. M., Russell, L. M., Jefferson, A., and Quinn, P. K., Arctic organic aerosol measurements show particles from mixed combustion in spring haze and from frost flowers in winter, Geophys. Res. Lett., 37, doi:10.1029/2010GL042831, L10803, 2010.

Swietlicki, E., Hansson, H. C., Hameri, K., Svenningsson, B., Massling, A., McFiggans, G., McMurry, P. H., Petaja, T., Tunved, P., Gysel, M., Topping, D., Weingartner, E., Baltensperger, U., Rissler, J., Wiedensohler, A., and Kulmala, M., Hygroscopic properties of submicrometer atmospheric aerosol particles measured with H-TDMA instruments in various environments – a review, Tellus B, 60, 432–469, 2008.

Teinila, K., Hillamo, R., Kerminen, V. M., and Beine, H. J.: Aerosol chemistry during the NICE dark and light campaigns, Atmos. Environ., 37, 563–575, 2003.

Wallace, J. M. and Hobbs, P. V.: Atmospheric Science – An Introductory Survey, Academic Press, Elsevier, 2006.

Wolff, E. W., Rankin, A. M., and Rothlisberger, R.: An ice core indicator of Antarctic sea ice production, Geophys. Res. Lett., 30, 2158, doi:10.1029/2003GL018454, 2003.

Title Page

Abstract | Introduction

Conclusions | References

Tables | Figures

◄◄ | ►►

◄ | ►

Back | Close

Full Screen / Esc

Printer-friendly Version

Interactive Discussion

Table 1. Concentrations ($ng\,m^{-3}$) of ions in the size-segregated aerosol samples collected.

| Date	ID	Size. µm	Cl	NO$_3$	SO$_4$	Total anions	Date	ID	Size. µm	Cl	NO$_3$	SO$_4$	Total anions	Date	ID	Size. µm	Cl	NO$_3$	SO$_4$	Total anions
5/3-7/3	P1-01	18	19.0	13.4	19.3	51.6	13/3-16/3	P4-01	18	3.6	3.0	2.4	8.9	20/3-22/3	P7-01	18	154.2	29.8	58.1	242.1
	P1-02	10	10.0	9.1	2.1	21.2		P4-02	10	2.4	2.0	<DG	4.3		P7-02	10	19.0	5.2	4.0	28.2
	P1-03	5.6	8.56	7.2	0.5	16.3		P4-03	5.6	2.3	2.6	1.5	6.4		P7-03	5.6	6.1	4.2	<DG	10.7
	P1-04	3.2	20.4	9.9	3.7	34.0		P4-04	3.2	4.2	3.6	1.4	9.2		P7-04	3.2	33.3	7.2	6.1	46.6
	P1-05	1.8	69.5	24.5	19.2	113.1		P4-05	1.8	10.5	9.4	7.6	27.5		P7-05	1.8	88.8	22.4	27.8	139.0
	P1-06	1	87.1	38.6	27.9	153.7		P4-06	1	10.2	12.5	12.9	35.6		P7-06	1	73.6	32.5	40.7	146.7
	P1-07	0.56	79.5	39.3	81.1	199.9		P4-07	0.56	8.7	16.4	83.1	108.2		P7-07	0.56	53.7	32.4	169.3	255.5
	P1-08	0.32	27.1	21.4	290.2	338.7		P4-08	0.32	2.9	4.3	427.1	434.3		P7-08	0.32	5.0	4.0	620.8	629.8
	P1-09	0.18	12.4	12.0	83.9	108.3		P4-09	0.18	2.6	6.3	136.6	145.5		P7-09	0.18	4.2	4.2	145.5	153.8
	P1-10	0.1	7.4	6.9	7.8	22.1		P4-10	0.1	2.2	2.5	13.3	18.0		P7-10	0.1	3.3	3.4	11.3	17.9
	P1-11	0.056	6.9	10.2	<DG	16.8		P4-11	0.056	3.4	2.3	2.3	7.9		P7-11	0.056	3.4	2.8	3.7	9.9
	Total		347.7	192.5	535.4			Total		53.0	64.9	688.0			Total		444.5	148.1	1087.6	
7/3-10/3	P2-01	18	14.5	6.8	9.6	30.9	16/3-17/3	P5-01	18	17.0	10.4	7.9	35.4	22/3-23/3	P8-01	18	27.7	2.6	5.1	35.4
	P2-02	10	7.4	2.4	9.1	18.9		P5-02	10	7.0	19.7	<DG	25.2		P8-02	10	10.6	6.1	<DG	15.6
	P2-03	5.6	2.2	1.7	<DG	3.3		P5-03	5.6	7.8	40.1	<DG	47.9		P8-03	5.6	17.6	<DG	<DG	13.4
	P2-04	3.2	4.4	5.4	1.5	11.3		P5-04	3.2	10.0	42.7	0.3	52.8		P8-04	3.2	33.2	<DG	6.7	40.9
	P2-05	1.8	15.1	12.3	11.1	38.5		P5-05	1.8	20.0	22.4	5.3	47.7		P8-05	1.8	82.7	22.5	30.4	135.5
	P2-06	1	24.0	20.5	17.7	62.2		P5-06	1	34.6	59.4	13.8	107.9		P8-06	1	57.5	28.1	39.1	124.6
	P2-07	0.56	45.2	47.7	82.1	175.1		P5-07	0.56	52.7	29.1	94.4	176.2		P8-07	0.56	27.9	20.6	179.6	228.1
	P2-08	0.32	10.9	13.6	316.0	340.5		P5-08	0.32	16.7	12.3	441.7	470.7		P8-08	0.32	6.9	10.8	605.1	622.8
	P2-09	0.18	4.5	5.3	106.1	115.9		P5-09	0.18	11.1	16.9	104.0	132.0		P8-09	0.18	7.2	<DG	122.8	125.4
	P2-10	0.1	2.2	2.0	11.44	15.7		P5-10	0.1	15.1	8.5	9.6	33.2		P8-10	0.1	11.8	<DG	8.0	14.0
	P2-11	0.056	4.4	5.8	1.81	12.0		P5-11	0.056	15.5	36.8	<DG	52.1		P8-11	0.056	8.2	<DG	<DG	1.3
	Total		134.8	123.4	565.9			Total		207.4	298.4	675.4			Total		291.3	70.9	994.8	
10/3-13/3	P3-01	18	12.7	5.6	9.4	27.6	17/3-20/3	P6-01	18	32.8	5.5	5.8	44.1	23/3-24/3	P9-01	18	11.6	<DG	<DG	5.3
	P3-02	10	3.2	1.6	0.3	5.1		P6-02	10	3.9	2.0	<DG	5.6		P9-02	10	8.5	<DG	<DG	1.9
	P3-03	5.6	4.2	1.6	<DG	5.8		P6-03	5.6	3.0	2.6	<DG	5.2		P9-03	5.6	7.0	<DG	<DG	7.8
	P3-04	3.2	21.1	6.4	7.6	35.1		P6-04	3.2	20.2	3.7	2.1	26.0		P9-04	3.2	15.1	6.0	5.9	27.0
	P3-05	1.8	80.9	23.0	37.6	141.5		P6-05	1.8	115.8	12.4	17.3	145.5		P9-05	1.8	22.0	4.9	16.4	43.3
	P3-06	1	78.7	31.6	57.3	167.6		P6-06	1	149.9	23.4	31.8	205.1		P9-06	1	16.8	4.6	20.5	41.9
	P3-07	0.56	48.6	23.0	160.0	231.6		P6-07	0.56	140.7	29.2	108.4	278.3		P9-07	0.56	10.9	<DG	111.1	121.2
	P3-08	0.32	17.2	6.7	473.5	497.5		P6-08	0.32	22.7	6.2	393.6	422.5		P9-08	0.32	8.9	<DG	321.0	328.0
	P3-09	0.18	10.3	6.9	175.0	192.2		P6-09	0.18	12.2	5.2	117.9	135.2		P9-09	0.18	8.1	4.1	70.0	82.2
	P3-10	0.1	3.4	2.5	22.0	27.9		P6-10	0.1	3.9	2.8	13.7	20.4		P9-10	0.1	11.4	<DG	36.3	46.3
	P3-11	0.056	2.5	2.1	7.0	11.7		P6-11	0.056	2.4	2.6	2.0	6.9		P9-11	0.056	8.7	<DG	22.7	29.6
	Total		282.9	111.0	949.6			Total		507.6	95.4	692.0			Total		129.1	2.1	603.4	
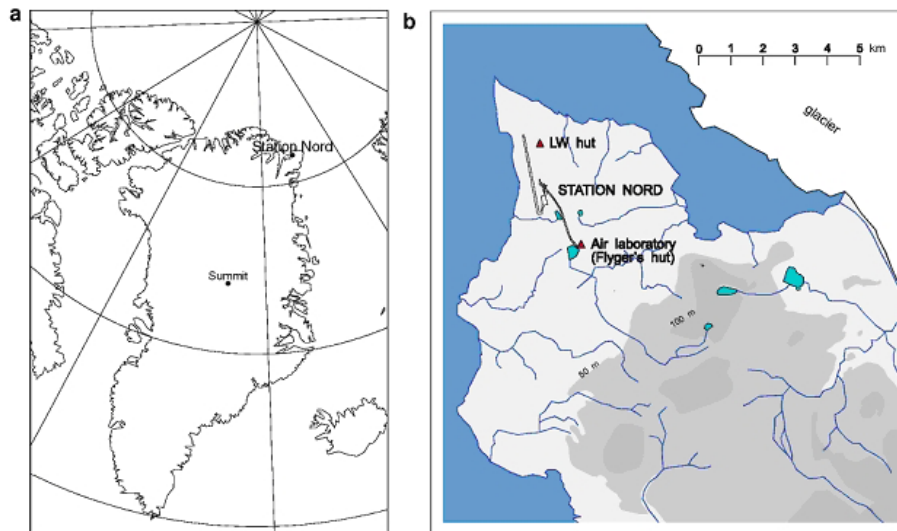
Fig. 1. (a) Greenland with the location of Station Nord and **(b)** the position of the air monitoring site Flyger's Hut at Station Nord (Heidam et al., 1999).
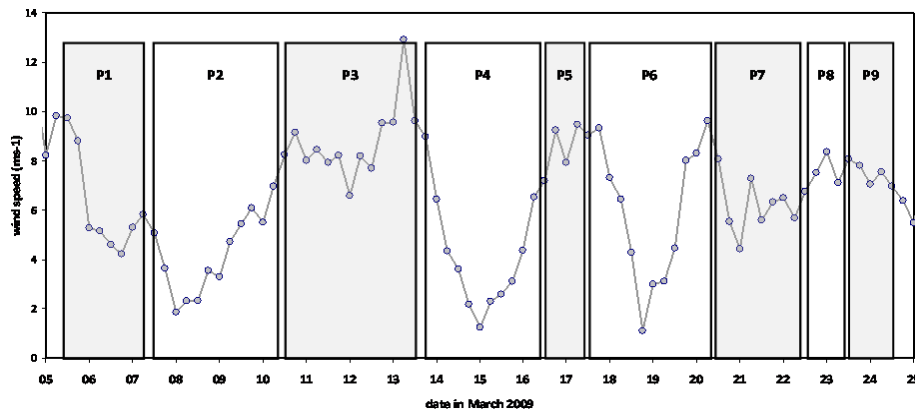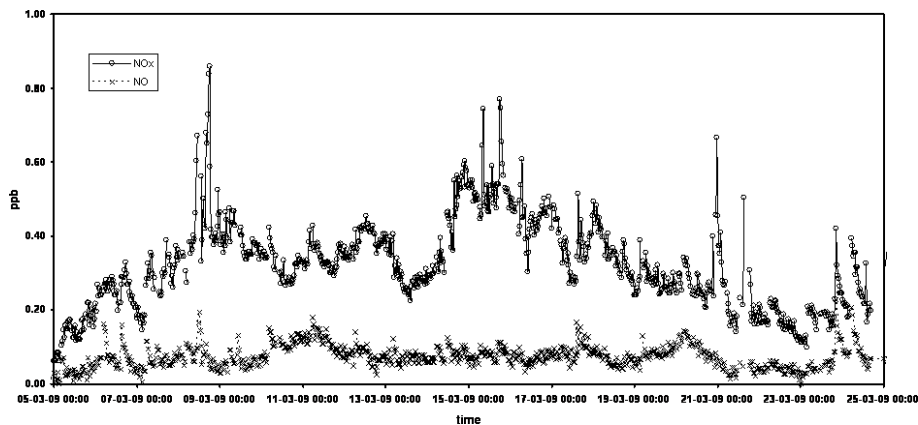
Fig. 2. 6 h wind speed at Long 16.5° W Lat 81.5° N during the field campaign in March 2009. The data are reanalysis data from NCEP/DOE AMIP II. The different sampling periods (Px) for aerosol sampling are shown.

Fig. 3. Atmospheric concentrations of NO and NO$_x$ at Station Nord measured as half hour mean during the field campaign in March 2009.
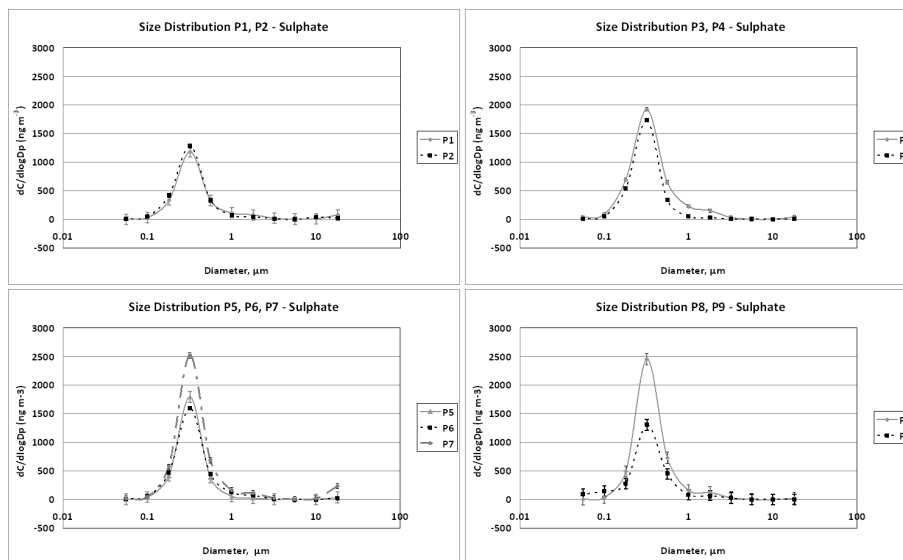
Fig. 4. Normalized size-segregated mass distribution of SO_4^{2-} during the sampling periods P1–P9.
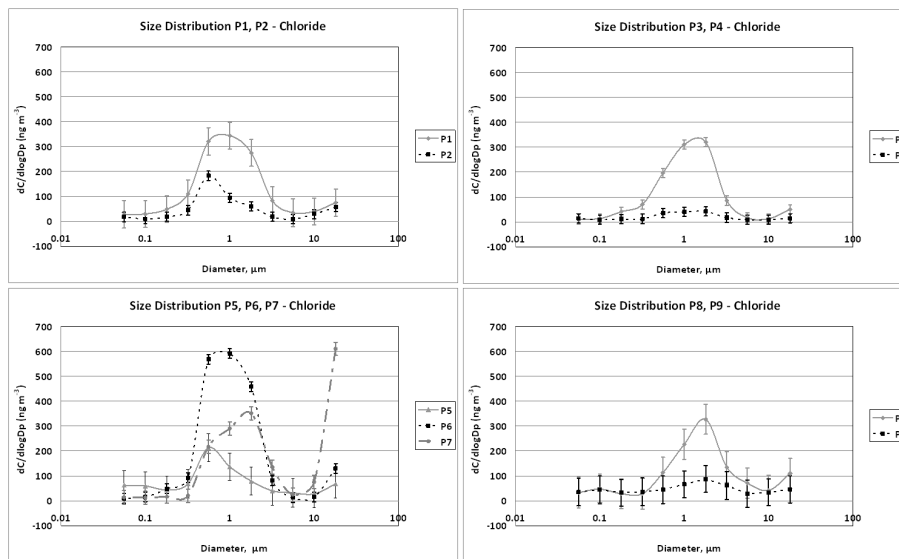
Fig. 5. Normalized size-segregated mass distribution of Cl⁻ during the sampling periods P1–P9.

Sources of anions in aerosols in northeast Greenland during late winter

M. Fenger et al.
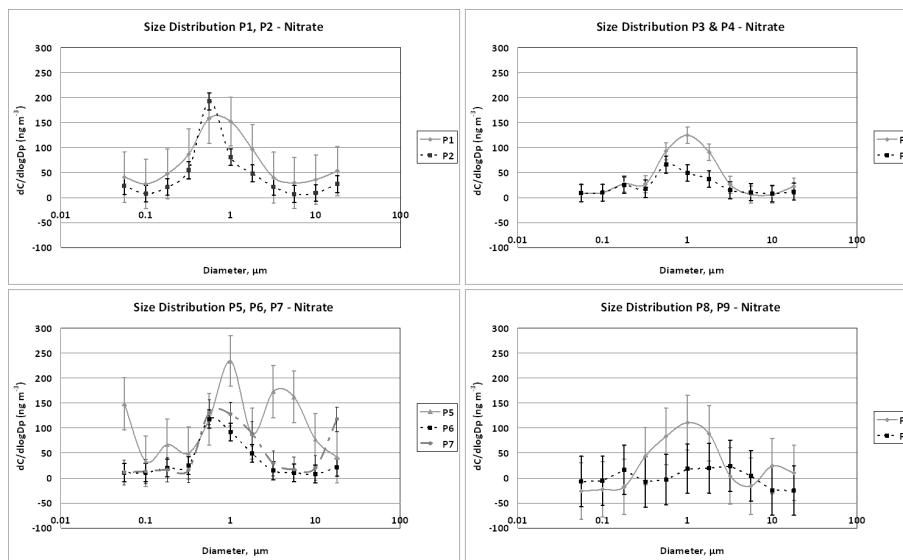
Fig. 6. Normalized size-segregated mass distribution of NO_3^- during the sampling periods P1–P9.
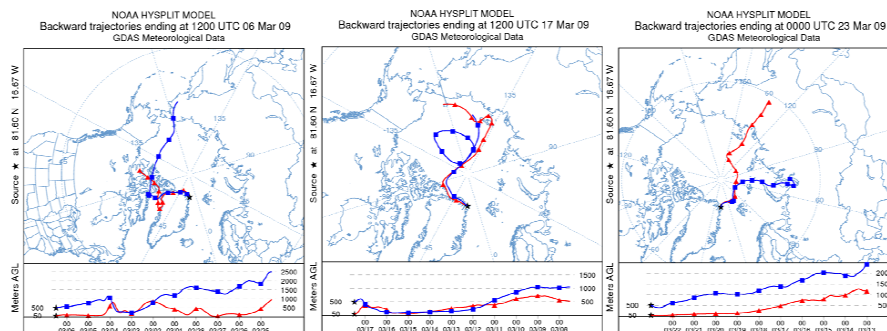
Fig. 7. Air mass back trajectories from the model HYSPLIT. The back trajectories are calculated for arrival at 50 m and 500 m a.s.l. every 12 h. The trajectories are shown for three typical cases: **(a)** west of Station Nord (Canada, West Greenland and the North Pole) **(b)** along the coast of North Greenland and **(c)** north of Station Nord (The North Pole and Siberia).
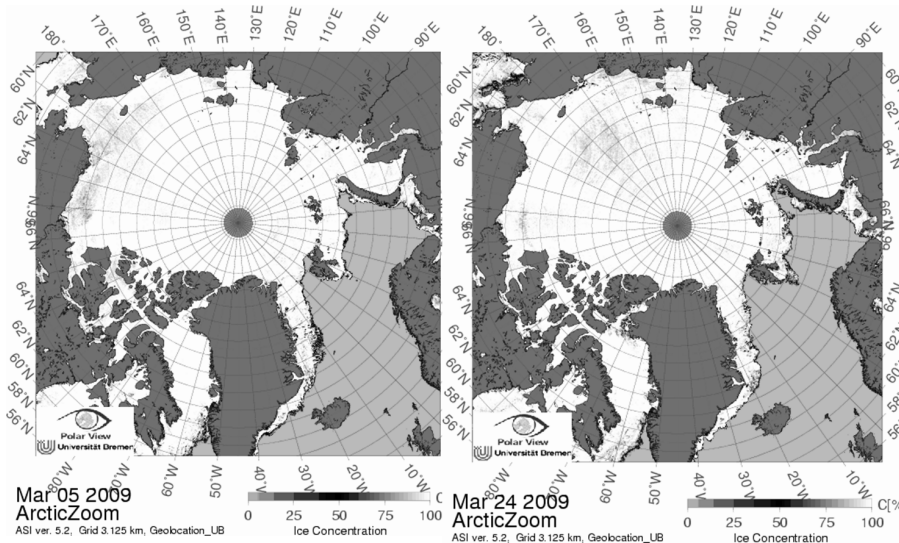
Fig. 8. Sea ice extension on 5 and 24 March 2009.